Journal of Modern Technology and Engineering
Vol.8, No.2, 2023, pp.84-95

Jomard Publishing

# UTILIZATION OF MRI AND HEMOGRAM DATA IN DIAGNOSIS OF ALZHEIMER'S DISEASE: COMPARISON OF VARIOUS DEEP LEARNING METHODS

**Adem Mert Akkaya**[1*], **Ömer Can Kuşcu**[1], **Korhan Günel**[2], **Ayşegül Metin**[1], **Yelda Özsunar**[3]

[1]Aydın Science High School, Aydın, Türkiye
[2]Department of Mathematics, Faculty of Science, Aydın Adnan Menderes University, Aydın, Türkiye
[3]Department of Radiology, Faculty of Medicine, Aydın Adnan Menderes University, Aydın, Türkiye

**Abstract.** Alzheimer's Disease (AD) is a progressive brain disorder affecting thinking, memory and behavior. It is the most common cause of dementia, leading to a decline in cognitive abilities due to the death of brain cells. This study aims to provide a new perspective on AD diagnosis by comparing innovative approaches and existing methods. The use of MRI enables non-invasive brain imaging, detecting subtle changes indicating Alzheimer's in brain structure. MRI data were used for training and testing Convolutional Neural Networks (CNNs) and Vision Transformer (ViT) models. Additionally, hemogram data's accessibility and comprehensive view may improve Alzheimer's diagnosis accuracy. Hemogram data were evaluated using K-Nearest Neighbors (KNN), Random Forest Classifier (RFC), Decision Tree Classifier (DTC), and Multi-Layer Perceptron (MLP) models. The best CNN model achieved 0.95 ACC (Accurracy) and 0.98 AUC (Area Under Curve) when trained on MRI data. The ViT model performed at 0.90 ACC and 0.92 AUC. The most successful model for hemogram data was KNN with an 0.83 ACC and 0.83 F1 Score. The prioritized parameters in the hemogram data, determined using the applied approaches, are listed in the following order: Lymphocytes, PCT, RDW, MCV, and Monocytes. It is believed that assessing hemogram data for Alzheimer's diagnosis and exploring the ViT model could offer novel insights to the literature.

**Keywords**: Machine learning in Health Sciences, Convolutional Neural Network, Vision Transformer, MRI, Neuroimaging, Clinical Decision Support.
**AMS Subject Classification:** 68T01, 68T05, 68Q32.
[*]**Corresponding author:** Adem Mert Akkaya, Aydın Science High School, Aydın, Türkiye,
e-mail: *ademmertakkaya1@gmail.com*
*Received: 14 February 2023; Revised: 13 April 2023; Accepted: 4 May 2023; Published: 31 August 2023.*

## 1 Introduction

In 2012, Dementia was declared a public health priority by the World Health Organization (WHO). Alzheimer's is the most common cause of dementia among older adults and its prevalence increases with age. According to a study published in the Journal of the American Medical Association (Hebert et al., 2013), the prevalence of Alzheimer's disease in adults aged 65 and older is estimated to be between 10-25%. Research has shown that by 2050, 22% of the world's population will be aged 60 and over, and as a result, the number of individuals with Alzheimer's disease will increase significantly, placing a considerable burden on healthcare systems (The Alzheimer's Association, 2023). The Alzheimer's Association's special report in 2023 provides

comprehensive statistics on the public health impact of Alzheimer's disease to clarify the current and future state. The report covers various aspects, including prevalence and incidence rates, mortality and morbidity figures, care utilization and costs, as well as the overall impact on family carers, the dementia workforce, and society as a whole (see The Alzheimer's Association (2023)).

The hospitalization cost for Alzheimer's and other dementia patients aged 65 and over is three times higher than for those without dementia, and the cost of care homes is twenty times higher (Lai, 2012). The onset and progression of Alzheimer's Disease (AD) can vary greatly between individuals, with early symptoms including memory loss, difficulty with language and communication, orientation problems, and changes in mood and behavior. As the disease progresses, individuals may experience severe memory loss, difficulty with daily activities, and a decline in physical function (Prince et al., 2013).

The increasing prevalence of Alzheimer's disease and its potential impact on healthcare systems have prompted researchers to delve deeper into the disease. While there is currently no cure, efforts are focused on managing symptoms and slowing the progression of the disease (Sperling et al., 2011). Research on Alzheimer's disease continues to focus on understanding the underlying causes of the disorder and developing new treatments, with studies suggesting that risk factors for Alzheimer's disease include genetic factors (Montine et al., 1997), lifestyle factors such as diet and exercise, and certain medical conditions such as hypertension and diabetes (Barnes & Yaffe, 2011).

The diagnosis of neurodegenerative diseases such as dementia, which significantly disrupts daily life, is essential through neuroimaging (Frisoni et al., 2003). In 2000, the European Federation of Neurological Societies and in 2001, the American Academy of Neurology reported that at least one imaging with CT or MRI should be performed in patients diagnosed with dementia to identify organic diseases that may cause dementia, such as tumors, stroke, normal pressure hydrocephalus, and subdural hematoma (Waldemar et al., 2000).

Magnetic Resonance Imaging (MRI) is a non-invasive diagnostic technique that uses a powerful magnetic field, radio waves, and a computer to produce detailed images of the internal structures of the body. MRI is particularly useful for imaging soft tissues that are difficult to visualize with other imaging techniques, such as the brain and spinal cord, as well as muscles and tendons. One of the main advantages of MRI is that it can produce high-resolution, multi-planar images without using ionizing radiation. This makes it a safe and effective imaging method for a wide range of applications, including the diagnosis of degenerative diseases such as brain tumors, stroke, and Alzheimer's disease. T2-weighted images, which are an example of the images that can be produced by MRI, are typically used to image soft tissues such as muscles and tendons. T2-weighted images provide good contrast between fluid-filled spaces such as cysts and tumors and the surrounding tissue as seen in Figure 1.

On the other hand, a hemogram, also known as a Complete Blood Count (CBC), is a series of tests performed on a blood sample to measure red blood cells, white blood cells, and platelets, as well as other parameters such as hemoglobin levels, and these tests are commonly used in the diagnosis and treatment of a wide variety of diseases and conditions, including anemia, leukemia, and infections. The CBC is widely used because it provides important information about a patient's overall health and can help doctors monitor the effectiveness of treatments (Complete Blood Count (CBC) - Mayo Clinic, 2023). While a hemogram is a valuable diagnostic tool for various medical conditions, it is not typically used as a primary test for diagnosing Alzheimer's disease. However, it plays a supportive role in the overall diagnostic process by providing valuable information about the patient's general health and ruling out other potential causes of cognitive decline.

The literature on the application of artificial intelligence-supported analysis techniques on these data is developing day by day. Various machine learning and deep learning techniques have been applied to these type of data in this study for diagnosing Alzheimer's disease.

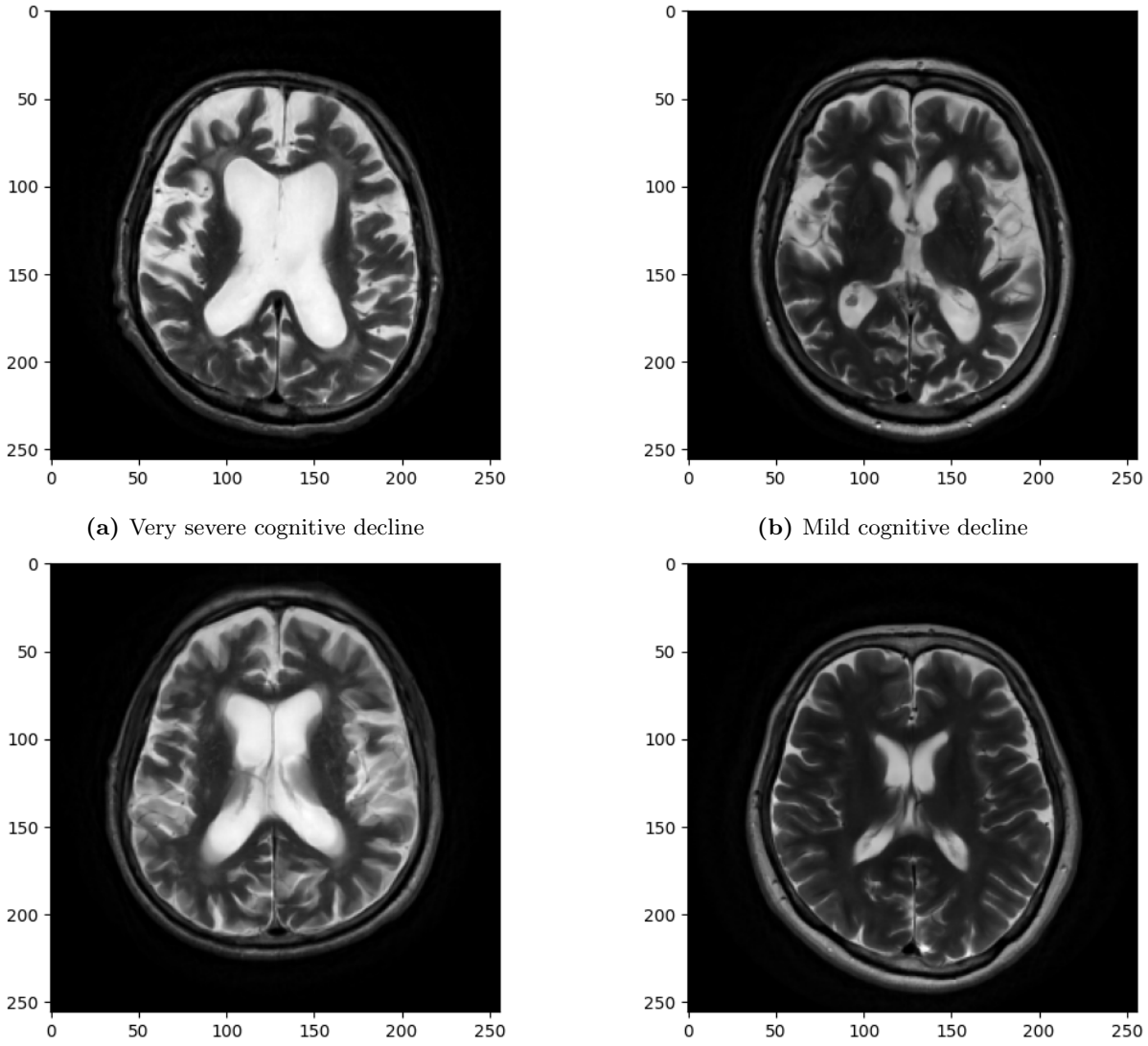

**(a)** Very severe cognitive decline

**(b)** Mild cognitive decline

**(c)** Moderate cognitive decline

**(d)** No cognitive impairment

**Figure 1:** Sample T2-weighted images for some patients examined by Aydın Adnan Menderes University.

In this study, MRG data was processed with two architectures. Convolutional Neural Networks (CNNs) have become a remarkably important algorithm in many fields, from image processing to speech recognition in recent years. The most significant feature of CNNs is that they reduce the number of parameters required for Artificial Neural Networks (Albawi et al., 2017). CNNs have a strong potential to be used in radiology for classification, segmentation, and lesion detection, which have become dominant in medical computer vision in recent years (Yamashita et al., 2000). CNNs consist of layers such as convolutional layers, pooling layers (Gu et al., 2018). As the name suggests, the convolutional layer plays the most important role in CNN. The filters, called kernels, which can learn the important points, are the focus of this layer. These layers, which are generally small matrices, slide over the input and calculate scalar products for the location they are in. These products are converted into matrices and given as the output of the layer (O'Shea & Nash, 2015).

Vision Transformer (ViT) is a state-of-the-art neural network architecture for image recognition tasks that has gained significant attention in the computer vision community. Unlike traditional CNNs, ViT employs a pure transformer-based architecture that can process images as sequences of tokens, eliminating the need for any pre-processing steps such as hand-crafted

feature extraction or data augmentation.

Machine learning techniques and MLP were applied to hemogram data. Machine learning is a subfield of artificial intelligence that enables computers to learn from data. The main idea behind machine learning is to develop models that can learn from new data and make predictions on different data in the future (Hastie et al., 2009). This is achieved through training the model on a dataset where the model's parameters are adjusted to optimize its performance. Once trained, the model can be applied to new data and used to make predictions or classify data based on the features learned during training (Alpaydin, 2009). Multilayer Perceptron (MLP) is a type of Artificial Neural Network (ANN) used for supervised learning tasks such as classification and regression. It consists of many layers of artificial neurons, typically organized as an input layer, one or more hidden layers, and an output layer. The input layer receives input data and the output layer produces the network's prediction. Each neuron in an MLP takes input from the previous layer, performs a mathematical operation on it, and produces an output that is passed to the next layer. The operation performed by each neuron is usually a linear combination of its inputs, followed by a nonlinear activation function. MLPs are trained using a technique called backpropagation, which adjusts the weights of the neurons based on the error between the predicted output and the true output. MLPs are widely used in various applications such as image recognition, natural language processing, and financial forecasting.

In aim of this study is to develop machine learning models to assist medical professionals in diagnosing of Alzheimer's disease (AD) based on MRI and Hemogram test data, and to investigate the accuracy of these models as a decision-making mechanism. For this aim, the rest of this paper is organized as follows. Firstly, data preprocessing steps, machine and deep learning model architectures used in this study have been described in Section 2. In Section 3, it is summarized how to achieve high accuracy metrics for MRI data, with CNN outperforming ViT, and identified key Hemogram parameters associated with Alzheimer's disease. This section also presents a discussion comparing the study's results with existing literature, emphasizing the advantages of different model architectures and the potential of combined MRG and Hemogram data for early diagnosis. Finally, the paper concludes the study's findings, highlighting the potential for using machine and deep learning models with MRG and Hemogram data in Alzheimer's disease diagnosis and suggesting areas for future research.

## 2 Materials and Method

The study has obtained ethical approval from the Adnan Menderes University Faculty of Medicine Non-Invasive Clinical Research Ethics Committee (Decision No: 2022/189, 8 December 2022). The data used in the study consists of anonymized tests of patients who applied to the hospital between September 1, 2012 and September 1, 2022.

The aim of this study is to contribute to the developing literature on the potential use of machine learning techniques with Magnetic Resonance Imaging (MRI) data as an alternative or complementary diagnostic tool for Alzheimer's disease, to investigate the potential use of hemogram data in AD diagnosis, and to contribute to the medical literature with the analyses conducted through the methods used.

The MRI data used in the study were labeled by radiologists. The hemogram data were labeled using past medical records. The MRI samples consist of 39 HCE (Healthy Elderly Control) and 39 AD diagnosed MRI samples with T2-weighted cranial sequence. The hemogram data for the HCE label were composed of 2787 hemogram test results with 22 parameters from patients aged 65 and over without any other diseases with R53 ICD 10 code. The hemogram data for the AD label were composed of 2787 test results with 22 parameters from patients with G30 and G30.9 ICD 10 code. Tests with missing parameters were not included in these data.

The MRI data used in the study were resized using anti-aliasing techniques to minimize data loss, with each slice having a resolution of 256x256 and each MRI consisting of 24 slices. A total

of 12 slices were removed from the top and bottom of each MRI. The total number of slices was 936, with each slice being separated to fit the architecture of the slice-based 2D models, and the grayscale brightness range of 0-255 was reduced to 0-1 using MinMax Scaling to process the MRI data.

In the study, age values were created from the given date of birth and test date values in the Hemogram data. Non-numeric data was converted to numeric using Label and OneHot encoding. The data, which originally had each value in a row and each test referenced by a barcode number, was processed to have each test in a row. Then, MinMax Scaling was applied to the parameters to scale them down to the range of 0-1.

The processed MRI data used in the study were divided into training-test sets in a ratio of 54-20. Hemogram data, on the other hand, were 80-20 percent in training-test sets. In order to prevent data leakage during this process, it was observed that the same patient data would not fall into different sets. At the same time, both the training and the test set were kept balanced. While label and image data were used in the training stage in the MRI data, only the image data was used in the testing stage. In the hemogram, excluding gender and age parameters, "Erythrocyte, MCV, Lymphocyte%, MPV, Eosinophil%, Hematocrit, MCH, Platelet, Basophil%, Monocyte%, Leukocyte, Lymphocyte#, Hemoglobin, MCHC, Neutrophil#, PDW, RDW, Eosinophil# , Basophil#, PCT, Neutrophil%, Monocyte#" and label data were used in the training stage.

In this study, two different models were trained for the MRI data using two different architectures. The first one is a CNN architecture. The best performing model had a input size of (174, 256, 256, 1) or (batch size, width, height, channel) and consisted of a 2D convolutional layer with 256 filters and a (3,3) kernel size, a MaxPooling layer with a (8,8) size, a 2D convolutional layer with 128 filters and a (3,3) kernel size, a MaxPooling layer with a (4,4) size, a Flatten layer, and 7 dense layers with (1024, 512, 256, 128, 64, 32, 1) artificial neurons. The ReLU activation function ($f(x) = \max(0, x)$) was used in all layers except for the last layer, where the sigmoid activation function $\left(f(x) = \frac{1}{1+e^{-x}}\right)$ was used. The Adadelta optimization function was used.

The second architecture used for the MRI data was the ViT. The best performing model had the same input size as the CNN architecture and consisted of a patch encoding with a (16,16) size, 4 Transformer layers, and 3 dense layers with (1024, 512, 1) artificial neurons. The Adadelta optimization function was also used in this model.

For the hemogram data, four different models were trained using different architectures. The first one was a Multilayer Perceptron (MLP) model consisting of 10 hierarchical layers with an input size of (24, batch size). The ReLU activation function was used in all layers except for the last layer, where the sigmoid activation function was used. The Adam Optimizer was used as the optimization function. In addition to MLP, K-Nearest Neighbors (KNN), Random Forest Classifier (RFC), and Decision Tree Classifier (DTC) models were also trained. Python 3.9, Tensorflow and Keras libraries were used for CNN, ViT, and MLP training, while the Scikit Learn library was used for KNN, RFC, and DTC training. The model weights were randomly initialized and then optimized. In addition, the Select From Model method from the Scikit Learn library was applied to the hemogram data.

According to the experiments conducted on 58 MRI samples (696 slices), the optimum hyperparameters for the CNN model were determined to be an epoch number of 150 and a batch size of 174. As for the ViT model, the hyperparameters were determined to be an epoch number of 100 and a batch size of 174.

The MLP and ML models were trained using 4459 hemogram data with hyper-parameters determined based on experiments. The KNN model had a K value of 3, while the MLP model had an epoch value of 125 and a batch size of 557 to get optimum results.

The ViT, CNN, MLP, and machine learning models trained were evaluated based on their accuracy metrics as well as their ability to generalize. To assess the CNN model's generalizability,

3-fold cross-validation was applied. Based on these evaluations, the recommended models were selected.

The CNN and ViT models were tested on 24 MRI samples (288 slices). Test results were evaluated using appropriate metrics in the literature such as ROC curve, Accuracy, and Confusion Matrix. The MLP and machine learning models were tested on 1115 hemogram test data. Test results were evaluated using appropriate metrics accepted in the literature such as $F_1$ score and Accuracy.

## 3 Results and Findings

In this study, MRG data consisted of tests from 39 HCE and 39 AD-diagnosed patients aged 65 and over. Hemogram data consisted of 2787 test results from patients aged 65 and over diagnosed with AD (ICD-10 codes G30 and G30.9) and 2787 test results from patients aged 65 and over without any other diseases (ICD-10 code R53). During the training stage, binary labels of AD and HCE were used.

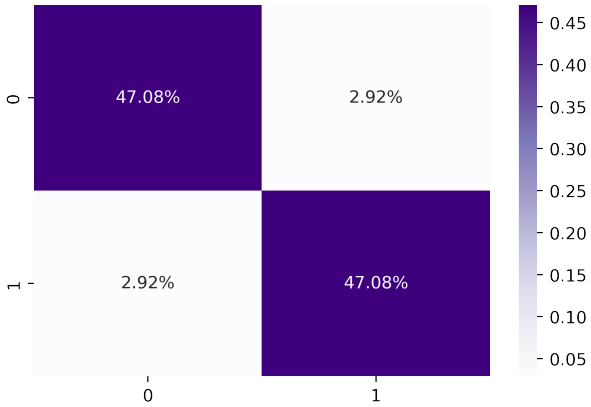


**Figure 2:** Confusion Matrix of 2D slice-based CNN Model

The CNN model developed in this study using machine learning techniques achieved an accuracy of 0.9416 on the test set and 0.95 on the validation set when applied to the MRG data (Figure 2).

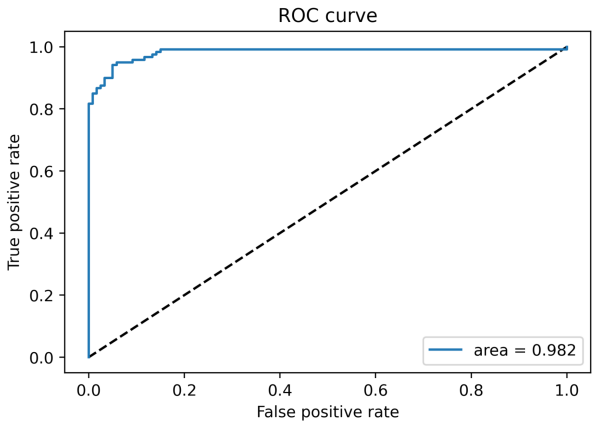


**Figure 3:** ROC Curve of 2D slice-based CNN Model

The area under the curve ($AUC$) value of the model was calculated as 0.982 (Figure 3). The 3-fold cross-validation standard deviation of the model was determined to be 0.019. Although the CNN model was trained on 2D slice-based MRG data, an approach was also tested where 12

slices of each MRG in the test set were evaluated to make a decision about the outcome. This approach accurately predicted all 20 MRGs in the test set with a standard deviation of 0 in the 3-fold cross-validation.

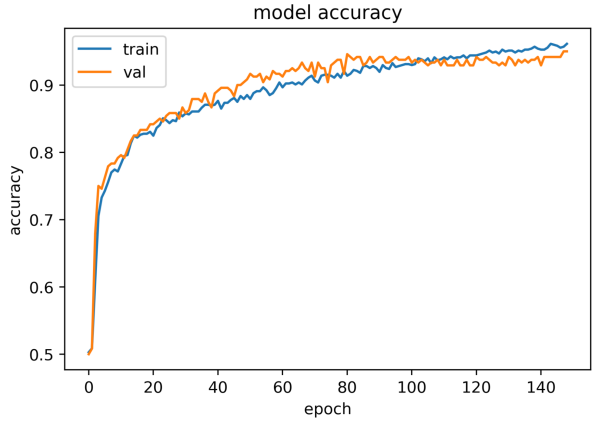


**Figure 4:** *ACC*-epoch Graph of 2D slice-based CNN Model

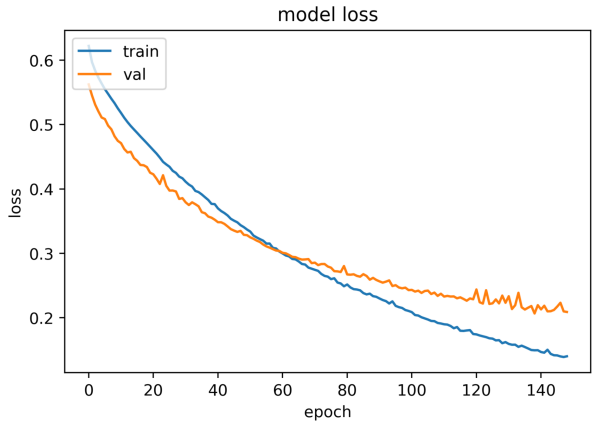


**Figure 5:** Loss-epoch Graph of 2D slice-based CNN Model

The acc-epoch, loss-epoch, and precision/recall-epoch graphs of the model were also created to evaluate the model's optimization (Figure 4, 5, 6).

In the study, in addition to the CNN model, the ViT (Vision Transformer) model was also trained with MRG data. The ViT model achieved an accuracy score of 0.92 and an *AUC* score of 0.90 on the test set. When evaluated with the voting method mentioned, the model correctly predicted 19 out of 20 examples in the test set. Additionally, heatmaps from the Transformer layers of this model were generated for MRG examples, which can be evaluated for medical analysis and verifiability.

**Table 1:** *ACC* and $F_1$ score metrics of models trained with Hemogram data

| **Model** | **$F_1$ Score** | **Accuracy** |
|---|---|---|
| MLP | 0.8181 | 0.8142 |
| Decision Tree Classifier | 0.7575 | 0.7623 |
| K-NN Classifier | 0.8387 | 0.8385 |
| Random Forest Classifier | 0.8230 | 0.8269 |

In this study, four models were trained with Hemogram data. The MLP model that gave the optimum result achieved an accuracy of 0.8142 and an $F_1$ score of 0.8181. The trained Decision

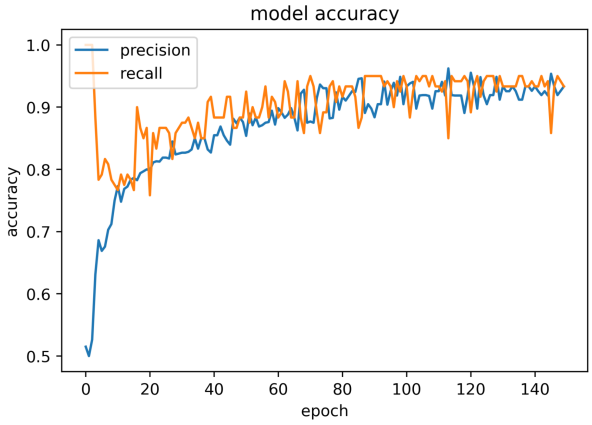


**Figure 6:** Precision/Recall-epoch Graph of 2D slice-based CNN Model

Tree Classifier model achieved an accuracy of 0.7623 and an $F_1$ score of 0.7575. The KNN Classifier achieved an accuracy of 0.8385 and an $F_1$ score of 0.8387, while the Random Forest Classifier achieved an accuracy of 0.8230 and an $F_1$ score of 0.8269 (Table 1). The proximity of $F_1$ score and accuracy values can be positively evaluated in terms of model performance and generalization ability. In addition, SelectFromModel feature selection was applied to the same data, and the data was shared according to the percentage of importance.

The use of advanced machine learning models with Magnetic Resonance Imaging (MRI) data for the diagnosis of Alzheimer's disease is a growing approach in the literature with the potential to improve the accuracy and speed of diagnosis. In this study, the proposed method enabled the combined use of MRI and Hemogram data in the diagnosis of Alzheimer's disease. Despite the extensive literature on image processing in Alzheimer's disease, studies on Hemogram data are quite limited.

**Table 2:** Metrics and Methodologies of Past Studies

| **Reference** | **Accuracy** | *AUC* | **Methodology** |
|---|---|---|---|
| Hinrichs et al. (2009) | 0.82 | 0.88 | Conventional classifiers (i.e. SVM, LPboosting) + voxel-level engineered features |
| Salvatore et al. (2015) | 0.76 | Unspecified | |
| Koikkalainen et al. (2011) | 0.86 | Unspecified | Conventional classifiers (i.e. linear regression, SVM) + region-level engineered features |
| Liu et al. (2016) | 0.93 | 0.96 | |
| Coupé et al. (2012) | 0.91 | Unspecified | Conventional classifiers (linear discriminant analysis, SVM) + patch-level engineered features |
| Liu et al. (2014) | 0.92 | 0.95 | |
| Tong et al. (2014) | 0.90 | Unspecified | |
| Suk et al. (2014) | 0.92 | 0.97 | Deep-Boltmann machine + patch-level engineered features |
| Liu et al. (2015) | 0.79 | 0.78 | Stacked auto-encoders + region-level engineered features |
| Shi et al. (2018) | 0.95 | 0.96 | Deep polynomial network + region-level engineered features |
| Korolev et al. (2017) | 0.80 | 0.87 | CNN + whole brain sMRI |
| Lian et al. (2020) | 0.90 | 0.95 | Hierarchical FCN + automatic discriminative localization |

The literature on using MRI data for Alzheimer's diagnosis has been reviewed. The study has achieved high accuracy metrics compared to the literature in binary classification, and has compared different feature engineering methods (patch-level, region-level) (Table 2). However, the study did not perform multi-class classification (i.e. AD-HCE-MCI) beyond binary classification. The study is open to improvement in this regard.

In the field of radiographic image processing, the use of CNNs is widespread. However,

there have been no studies in the literature that utilize the Vision Transformer architecture for the diagnosis of Alzheimer's disease. Image processing models based on these two different architectures were trained using MRG data. The advantage of the CNN architecture is its superiority in different metrics with a 0.95 Accuracy ($ACC$) and 0.98 $AUC$ value (Figure 2, 3). On the other hand, the ViT architecture stands out with its ability to provide medical interpretation through the analysis of heat map outputs from the attention layers, and the efficiency it would provide if the study is repeated on larger datasets.

**Table 3:** Certain Hemogram Parameters' Percent Significance by Analysis Result

| **Parameter** | **Percent Significance by Analysis Result**(%) |
|---|---|
| Lymphocyte# | 8.08 |
| PCT | 7.22 |
| RDW | 5.58 |
| MCV | 5.42 |
| Monocyte# | 5.39 |

Feature selection algorithms are important for interpreting data and for training models. In this study, the "SelectFromModel" method, which is one of these algorithms, was used to obtain results on the order of relevance of Hemogram parameters with Alzheimer's disease. The findings of the "SelectFromModel" model trained on Hemogram data identified the Hemogram parameters most strongly associated with Alzheimer's disease (Table 3). Future studies examining these parameters could yield important results for the diagnosis and treatment of Alzheimer's disease.

In the decision-making process, physicians analyze many variables crosswise. Converting raw data into qualified data facilitates this process for physicians. The combined analysis of Hemogram and MRG data can contribute to the early diagnosis of the disease. To explore this potential for early diagnosis, Mild Cognitive Impairment labeled data can be added to the dataset for further analysis.

In the literature, models trained with 2D (slice-based) or 3D (whole brain) architectures can be found for MRG analysis. While 2D models have advantages such as efficiency due to the ability to produce results from a single slice, 3D models have advantages such as a holistic approach. Although a 2D architecture was used in our study, a holistic approach was also tested by evaluating the results of slices throughout the MRG. It was observed that the approach of evaluating the entire MRG and reaching a conclusion for the patient achieved higher metrics compared to the results of the 2D slice-based model.

# 4 Conclusion

Alzheimer's disease is a cognitive disorder that is increasingly prevalent in our society and has a significant impact on the quality of life of patients as it progresses. In addition to radiographic examinations conducted by physicians, cognitive tests such as NINCDS-ADRDA are also used in the diagnosis of AD. The aim of this study was to diagnose Alzheimer's disease using easily obtained data such as MRG and Hemogram through various ML and DL models. CNN and ViT models were trained for MRG data, and the best model achieved an $ACC$ value of 0.95. MLP and various ML models were trained for Hemogram data, and the best model achieved an $ACC$ value of 0.83. Moreover, we also explored the use of hemogram data applying feature selection for Alzheimer's diagnosis, and outputs such as heatmaps from the region of interest were extracted to contribute to medical literature and future studies. Four different models were trained using different architectures, including Multilayer Perceptron (MLP), K-Nearest

Neighbors (KNN), Random Forest Classifier (RFC), and Decision Tree Classifier (DTC). The MLP model achieved an accuracy of 0.814 and an $F_1$ score of 0.818 on the test set.

The combined analysis of MRI and hemogram data showed promising results, indicating the potential for early diagnosis and improved decision-making for physicians. While this study has provided encouraging results, it also presents opportunities for future research. The inclusion of Mild Cognitive Impairment (MCI) labeled data in the dataset could further enhance the study's potential for early diagnosis. Additionally, exploring larger datasets and different machine learning architectures may yield even more accurate and generalized models for Alzheimer's disease diagnosis.

In conclusion, we believe that these results will contribute to the evolving literature and future studies, and will help improve the diagnosis of Alzheimer's disease and contribute to the well-being of patients and their families.

## 5 Acknowledgement

The authors would like to acknowledgement the support of Aydın Adnan Menderes University and staff. Special thanks are extended to Aslıhan Büyüköztürk Karul for her significant contributions to this study.

## Author Contributions

A.M. Akkaya and Ö.C. Kuşcu conceived of the proposed idea. K. Günel, A. Metin, and Y. Özsunar supervised the project. A.M. Akkaya and Ö.C. Kuşcu collected and verified the data. A.M. Akkaya and Ö.C. Kuşcu developed the pipeline and implemented the related codes together. A.M. Akkaya and Ö.C. Kuşcu carried out the results of the experiments. K. Günel, A.M. Akkaya, and Ö.C. Kuşcu wrote to this manuscript.

## References

Albawi, S., Mohammed, T.A. & Al-Zawi, S. (2017). Understanding of a convolutional neural network. 2017 International Conference on Engineering and Technology (ICET). doi: 10.1109/icengtechnol.8308186.

Alpaydin, E. (2010). *Introduction to Machine Learning* (Adaptive Computation and Machine Learning seriesş) (Second edition). The MIT Press.

Barnes, D.E. & Yaffe, K. (2011). The projected effect of risk factor reduction on Alzheimer's disease prevalence. *The Lancet Neurology*, *10*(9), 819-828. doi: 10.1016/s1474-4422(11)70072-2

Complete blood count (CBC) - Mayo Clinic. (2023, January 14). Complete Blood Count (CBC). (https://www.mayoclinic.org/tests-procedures/complete-blood-count/about/pac-20384919)

Coupé, P., Eskildsen, S.F., Manjón, J.V., Fonov, V.S., Pruessner, J.C., Allard, M., Collins, D.L. & Alzheimer's Disease Neuroimaging Initiative (2012). Scoring by nonlocal image patch estimator for early detection of Alzheimer's disease. *NeuroImage Clinical*, *1*(1), 141–152. doi: 10.1016/j.nicl.2012.10.002

Frisoni, G.B., Scheltens, Ph., Galluzzi, S., Nobili, F.M., Fox, N.C., Robert, P.H., Soininen, H., Wahlund, L.O., Waldemar, G. & Salmon, E. (2003) Neuroimaging tools to rate regional atrophy, subcortical cerebrovascular disease, and regional cerebral blood flow and metabolism: consensus paper of the EADC. *J Neurol Neurosurg Psychiatry*, *74*(10), 1371-81. doi: 10.1136/jnnp.74.10.1371

Gu, J., Wang, Z., Kuen, J., Ma, L., Shahroudy, A., Shuai, B., Liu, T., Wang, X., Wang, G., Cai, J. & Chen, T. (2018). Recent advances in convolutional neural networks. *Pattern Recognition*, *77*, 354–377. doi: 10.1016/j.patcog.2017.10.013

Hastie, T., Tibshirani, R. & Friedman, J. (2009). *The Elements of Statistical Learning: Data Mining, Inference, and Prediction*. Second Edition (Springer Series in Statistics), Springer New York, NY. doi: 10.1007/978-0-387-84858-7

Hebert, L.E., Weuve, J., Scherr, P.A. & Evans, D.A. (2013). Alzheimer disease in the United States (2010-2050) estimated using the 2010 census. *Neurology*, *80*(19), 1778–1783. doi: 10.1212/wnl.0b013e31828726f5

Hinrichs, C., Singh, V., Mukherjee, L., Xu, G., Chung, M.K., & Johnson, S.C. (2009) Alzheimer's Disease Neuroimaging Initiative. Spatially augmented LPboosting for AD classification with evaluations on the ADNI dataset. *Neuroimage*, *48*(1), 138-49. doi: 10.1016/j.neuroimage.2009.05.056

Koikkalainen, J., Lötjönen, J., Thurfjell, L., Rueckert, D., Waldemar, G., Soininen, H., & Alzheimer's Disease Neuroimaging Initiative (2011). Multi-template tensor-based morphometry: application to analysis of Alzheimer's disease. *NeuroImage*, *56*(3), 1134–1144. doi: 10.1016/j.neuroimage.2011.03.029

Korolev, S., Safiullin, A., Belyaev M. & Dodonova, Y. (2017). Residual and plain convolutional neural networks for 3D brain MRI classification. *2017 IEEE 14th International Symposium on Biomedical Imaging (ISBI 2017)*, Melbourne, VIC, Australia, 835-838, doi: 10.1109/ISBI.2017.7950647.

Lai, D.W.L. (2012). Effect of Financial Costs on Caregiving Burden of Family Caregivers of Older Adults. *SAGE Open*, *2*(4). doi: 10.1177/2158244012470467

Lian, C., Liu, M., Zhang, J. & Shen, D. (2020). Hierarchical Fully Convolutional Network for Joint Atrophy Localization and Alzheimer's Disease Diagnosis Using Structural MRI. *IEEE Trans. Pattern Anal. Mach. Intell.*, *42*(4), 880–893. doi: 10.1109/TPAMI.2018.2889096

Liu, M., Zhang, D., Shen, D. & Alzheimer's Disease Neuroimaging Initiative (2014). Hierarchical fusion of features and classifier decisions for Alzheimer's disease diagnosis. *Human brain mapping*, *35*(4), 1305–1319. doi: 10.1002/hbm.22254

Liu, S., Liu, S., Cai, W., Che, H., Pujol, S., Kikinis, R., ... & Fulham, M.J. (2014). Multimodal neuroimaging feature learning for multiclass diagnosis of Alzheimer's disease. *IEEE Transactions on Biomedical Engineering, 62*(4), 1132-1140. doi: 10.1109/TBME.2014.2372011

Liu, M., Zhang, D., & Shen, D. (2016). Relationship Induced Multi-Template Learning for Diagnosis of Alzheimer's Disease and Mild Cognitive Impairment. *IEEE transactions on medical imaging*, *35*(6), 1463–1474. doi: 10.1109/TMI.2016.2515021

Montine, K.S., Kim, P.J., Olson, S.J., Markesbery, W.R. & Montine, T.J. (1997). 4-hydroxy-2-nonenal pyrrole adducts in human neurodegenerative disease. *Journal of Neuropathology and Experimental Neurology*, *56*(8), 866–871. doi: 10.1097/00005072-199708000-00004

O'Shea, K., Nash, R. (2015). An Introduction to Convolutional Neural Networks. ArXiv. /abs/1511.08458. doi: 10.48550/arXiv.1511.08458

Prince, M., Bryce, R., Albanese, E., Wimo, A., Ribeiro, W., & Ferri, C.P. (2013). The global prevalence of dementia: a systematic review and metaanalysis. *Alzheimer's & Dementia, 9*(1), 63-75. doi: 10.1016/j.jalz.2012.11.007

Salvatore, C., Cerasa, A., Battista, P., Gilardi, M. C., Quattrone, A., & Castiglioni, I. (2015). Magnetic resonance imaging biomarkers for the early diagnosis of Alzheimer's disease: A machine learning approach. *Frontiers in Neuroscience*, *9*, 144798. doi: 10.3389/fnins.2015.00307

Shi, J., Zheng, X., Li, Y., Zhang, Q., & Ying, S. (2018). Multimodal Neuroimaging Feature Learning With Multimodal Stacked Deep Polynomial Networks for Diagnosis of Alzheimer's Disease. *IEEE Journal of Biomedical and Health Informatics*, *22*(1), 173–183. doi: 10.1109/JBHI.2017.2655720

Sperling, R.A., Aisen, P.S., Beckett, L.A., Bennett, D.A., Craft, S., Fagan, A.M., Iwatsubo, T., Jack, C.R., Jr, Kaye, J., Montine, T.J., Park, D.C., Reiman, E.M., Rowe, C C., Siemers, E., Stern, Y., Yaffe, K., Carrillo, M.C., Thies, B., Morrison-Bogorad, M., Wagster, M.V. & Phelps, C.H. (2011). Toward defining the preclinical stages of Alzheimer's disease: recommendations from the National Institute on Aging-Alzheimer's Association workgroups on diagnostic guidelines for Alzheimer's disease. *Alzheimer's & Dementia*, *7*(3), 280–292. doi: 10.1016/j.jalz.2011.03.003

Suk, H.I., Lee, S.W., Shen, D. & Alzheimer's Disease Neuroimaging Initiative. (2014). Hierarchical feature representation and multimodal fusion with deep learning for AD/MCI diagnosis. *NeuroImage*, *101*, 569–582. doi: 10.1016/j.neuroimage.2014.06.077

The Alzheimer's Association (2023). 2023 Alzheimer's disease facts and figures. *Alzheimer's Dement.*, *19* 1598-1695. doi: 10.1002/alz.13016

Tong, T., Wolz, R., Gao, Q., Guerrero, R., Hajnal, J. V., Rueckert, D. & Alzheimer's Disease Neuroimaging Initiative (2014). Multiple instance learning for classification of dementia in brain MRI. *Medical image analysis*, *18*(5), 808–818. doi: 10.1016/j.media.2014.04.006

Waldemar, G., Dubois, B., Emre, M., Scheltens, P., Tariska, P. & Rossor, M. (2000). Diagnosis and management of Alzheimer's disease and other disorders associated with dementia. The role of neurologists in Europe. European Federation of Neurological Societies. *European Journal of Neurology*, *7*(2), 133–144. doi: 10.1046/j.1468-1331.2000.00030.x

Yamashita, R., Nishio, M., Do, R.K.G. et al. (2018). Convolutional neural networks: an overview and application in radiology. *Insights Imaging*, *9*, 611–629. doi: 10.1007/s13244-018-0639-9